# Left ventricular myocardial deformation pattern, mechanical dispersion, and their relation with electrocardiogram markers in the large population-based STANISLAS cohort: insights into electromechanical coupling

Mario Verdugo-Marchese, Stefano Coiro, Christine Selton-Suty, Masatake Kobayashi, Erwan Bozec, Zohra Lamiral, Clément Venner, Faiez Zannad, Patrick Rossignol, Nicolas Girerd, et al.

# Left Ventricular Myocardial Deformation Pattern, Mechanical Dispersion and Their Relation with ECG Markers in The Large Population-Based Stanislas Cohort: Insights into Electro-Mechanical Coupling

Mario Verdugo-Marchese[1] MD, MSc; Stefano Coiro[2,3] MD, MSc; Christine Selton-Suty[4] MD; Masatake Kobayashi[2] MD; Erwan Bozec[2] PhD; Zohra Lamiral[2] , Clément Venner[4] MD, MsC; Faiez Zannad[2] MD, PhD; Patrick Rossignol[2]MD, PhD, Nicolas Girerd[2] MD, PhD; Olivier Huttin[2,4]MD, PhD.

[1] Département coeur-vaisseaux, Centre Hospitalier Universitaire Vaudois (CHUV), Lausanne, Switzerland.

[2] Université de Lorraine, INSERM, Centre d'Investigations Cliniques Plurithématique 1433, CHRU de Nancy, Inserm U1116, Nancy, France and FCRIN INI-CRCT (Cardiovascular and Renal Clinical Trialists) network, Nancy, France

[3] Division of Cardiology, University of Perugia, Ospedale S. Maria della Misericordia, Perugia, Italy

[4] Service de Cardiologie, Institut Lorrain du Cœur et des Vaisseaux, Centre Hospitalier Universitaire de Nancy

**Short title**: LV electromechanical coupling and myocardial deformation

**Keywords**: Myocardial deformation; Left ventricle; systolic function; Speckle-tracking echocardiography; Population study; Mechanical dispersion; Electromechanical coupling.

**Corresponding author**: Mario Verdugo-Marchese; mario.verdugo-marchese@chuv.ch.

**SOURCES OF FUNDING**: The STANISLAS study was sponsored by the Nancy CHRU and supported by a public grant overseen by the French National Research Agency (ANR) as part of the second "Investissements d'Avenir" programme (reference: ANR-15-RHU-0004), by the French PIA project «Lorraine Université d'Excellence » GEENAGE (ANR-15-IDEX-04-LUE) program, the Contrat de Plan Etat Région Lorraine and FEDER IT2MP, and a French Ministry of Health (Programme Hospitalier de Recherche Clinique Inter-régional 2008 - 2013) grant.

**Conflicts of interest**: Patrick Rossignol: Personal fees (consulting) from Novartis, NovoNordisk, Relypsa, AstraZeneca, Grünenthal, Idorsia, Stealth Peptides, Fresenius, Vifor; lecture fees from Bayer and CVRx; cofounder of CardioRenal.

**ACKNOWLEDGEMENTS**

Shown in **Supplementary material**

**ABSTRACT**

**BACKGROUND**: Mechanical alterations in patients with electrical conduction abnormalities are reported to have prognostic value in patients with left ventricular asynchrony or long QT syndrome beyond ECG variables. Whether conduction and repolarization patterns derived from ECG are associated with speckle tracking echocardiography (STE) parameters in subjects without overt cardiac disease is yet to be investigated.

**OBJECTIVES:** To report ranges of longitudinal deformation according to conduction and repolarization values in a population-based cohort.

**METHODS:** 1140 subjects (48.6±14.0 years, 47.7% men) enrolled in the 4$^{th}$ visit of the STANISLAS cohort (Lorraine, France) were studied. Echocardiography strain was performed in all subjects. RR, PR, QRS and QT intervals were retrieved from digitalized twelve-lead ECG. Echocardiographic data were stratified according to quartiles of QRS and QTc duration values.

**RESULTS:** Full-wall global longitudinal strain (GLS) was -21.1%±2.5% with a mechanical dispersion value of 33.6±11.7ms. Absolute GLS value was lower in the longest QRS quartile and shortest QTc quartile (both $p<0.001$). Time-to-peak of strain was not significantly different according to QRS duration although significantly higher in patients with higher QTc ($p<0.001$). Mechanical dispersion was significantly greater in patients with longer QTc (32.4±11.7ms for QTc<396ms versus 35.8±11.9ms for QTc>421ms; $p=0.002$).

**CONCLUSIONS:** Longer QTc is related to increased MD and better longitudinal strain values. In a population-based setting, QRS is not associated with MD, suggesting that echocardiography-based dyssynchrony does not largely overlap with ECG-based dyssynchrony.

**Introduction**

Electrical conduction in the heart and cardiomyocyte depolarization culminates in mechanical contraction (excitation-contraction coupling) (1). Pathological alterations in magnitude and timing of myocardial activity result in alterations in electrocardiogram (ECG) recordings. These subtle electrical variations should logically be translated into mechanical variations.

Left ventricular ejection fraction (LVEF) has long been the main biomarker for sudden cardiac death (SCD) risk assessment and therapeutic decision-making (2) although its accuracy has recently been questioned (3,4). Intraventricular conduction (QRS) delay and dispersion are linked to an increased risk of arrhythmia in a myriad of heart diseases (5,6) and are typically assessed by QRS duration and QT.

Speckle tracking echocardiography (STE) can identify subtle mechanical alterations of the myocardium affected by fibrosis and electrical conduction disturbances (7). In healthy subjects, peak longitudinal strain of the different LV segments occurs almost simultaneously with aortic valve closure (AVC), with no or only mild post-systolic shortening and a minimum of mechanical dispersion (MD). In addition, global longitudinal strain (GLS) has become the most robust STE-derived parameter in the prognostic assessment of patients with heart failure and reduced LVEF, dyssynchrony, and SCD (8,9). There is moreover growing evidence supporting the usefulness of temporal deformation parameters (e.g.MD) in predicting outcomes in both ischemic heart disease (10–12), and heart failure (13) as well as in selecting responders to resynchronization therapy (14,15).

While the value of ECG and STE variables has previously been evaluated, their interdependence has not been extensively assessed. Importantly, there is no published threshold in patients without cardiovascular disease and our knowledge of electromechanical coupling is mainly focused on patients with overt cardiac disease. The aims of the present study are to: i) investigate the association between intraventricular conduction delay and delayed repolarization (as assessed by QRS and QTc durations) with that of myocardial deformation profile and dispersion assessed by STE strain analysis, and ii) provide reference values of STE variables according to ECG variables in an initially healthy subjects.

## Methods

### Study population

The STANISLAS cohort is a single-center familial longitudinal cohort including 1006 families (4295 subjects) from the Nancy region who were recruited in 1993–1995 at the Center for Preventive Medicine (16). The subjects were of French origin and initially healthy, free of acute or chronic diseases (such as hypertension, diabetes, stroke, cancer, etc.). In the latest assessment performed in 2011–2016, a total of 1140 participants (aged 20 to 75 years with no evidence of cardiac disease) who had available echocardiographic images suitable for strain analysis was included in the current analysis (**Figure S1**). Details of the cohort investigations and loss to follow-up are provided in the Supplemental Digital Content (http://links.lww.com/HJH/A947) and have been published. The research protocol was approved by the local Ethics Committee and all study participants gave written informed consent. Clinical evaluation included information regarding past medical history, symptoms suggestive of any cardiovascular illness, anthropometric measurements (height, weight, and waist circumference), and general physical examination (including blood pressure measurement).

### Two-dimensional standard echocardiography

Examinations were performed in the left lateral decubitus position with a commercially available standard ultrasound scanner (Vivid 9, General Electric Medical Systems, Horten, Norway) using a 2.5MHz phased-array transducer (M5S). All echocardiographic and Doppler images were recorded in digital raw-data format and, after performing the centralized anonymization, submitted to the central core laboratory of the Centre d'Investigation Clinique (University of Lorraine, Nancy). Echocardiographic images were obtained from the 3 standard LV apical views (4-, 2- and 3-chambers). All images were acquired at a frame rate of 50 to 70 frames per second for two-dimensional views and at least three consecutive cardiac cycles were recorded.

### Post-processing analysis of deformation parameters

All strain measurements were performed offline by 2 experienced echocardiographers (OH, SC) with dedicated automated software (Q analysis software, Echo PAC PC version 110.1.0, GE Healthcare). This software enables real-time assessment of strain and strain rate, allowing a very rapid and simple analysis of deformation, by manually placing 3 sample points along the endocardium to define the LV base and the apex on an end-systolic frame and mid-wall myocardial layer strain (equivalent to full-wall) was obtained. Each LV wall was divided into 3 segments (basal, mid and apical), and the quality of tracking was assessed for each myocardial segment. Tracking feasibility in each apical view was rated on visual inspection. All echocardiographic studies with difficult images and/or moderate to poor tracking quality (n=415) were reviewed by a second senior echocardiographer. Segments or views with persistent poor tracking quality were excluded. Reproducibility analyses showed that inter and intra-observer reproducibility was good, with intra-class correlations >0.70 for all considered parameters (17).

**Strain parameters**

LV systolic deformation was assessed using the 3 apical views, with the following parameters derived from strain curves measured for each segment: 1) GLS, corresponding to the maximal absolute value of strain during ejection phase (before AVC), 2) end-systolic strain (ESS), corresponding to the value of strain at end-systole and 3) post-systolic strain (PSS), as the maximal absolute value of strain after AVC during the isovolumic relaxation phase. Post-systolic index (PSI) was automatically calculated by the software as (PSI=100*(PSS-ESS)/PSS), with a value ≥ 8 considered as abnormal.

The time from the beginning of the QRS to the peak early positive (P) systolic (S) and global (G) strain was automatically calculated by the software for each segment from which mean values and standard deviation were subsequently calculated for all patients. A bull's eye representation of these values was obtained (**Figure 1**). Global values were calculated by averaging all of the values computed at each segmental level from the same frame. To avoid confusion in terminology, a better strain means that the numerical value becomes increasingly negative, while a worst longitudinal strain is observed when LV function deteriorates and GLS becomes less negative. Transmural GLS (GSfull-wall) were automatically displayed and calculated from the average of all 17 segments. (**Figure 1 & 2**)

**Electrocardiographic recording**

ECGs were recorded at 25 mm/s with an amplification of 0.1 mV/mm in the supine position during quiet respiration and interpreted by a cardiologist. A well-defined protocol for electrode placement was used throughout the study. The RR, PR, and QRS intervals were measured in lead II to the nearest 2 ms from the averaged. Heart rate was calculated using the 1/RR interval. QT interval was measured in lead II or V5 (whichever provided the best delineation of the T wave), with the highest value defined as QTm (QT measured). Using the preceding RR interval, correction of the QT (QTc) interval was obtained by Fridericia's formula ($QTcF=QTm/\sqrt{RR^3}$) (18).

**Statistical methods**

Myocardial deformation parameters were stratified by the quartiles of QRS duration and QTc interval. Mean values of standard echocardiographic parameters, main deformation parameters and temporal deformation parameters were respectively compared between each quartile. Continuous variables are expressed as mean ± SD or median and $25^{th}$-$75^{th}$ percentiles as appropriate. Histograms and normal-quantile plots were visually inspected to verify the normality of distribution of continuous variables. GLS parameters were normally distributed. Correlation between QRS and QTc delays and STE-derived parameters was evaluated using the Spearman non-parametric method. In order to visualize and to interpret the differences of parameters between Qrs or Qt quartiles separately, radar charts were built using z-scores calculated from mean values of each parameter according to quartiles. P values $<0.05$ were considered to be statistically significant.

**Results**

**General characteristics**

On average, subjects were middle-aged (age 48.6±14.0 years) and overweight (BMI 25.5± 4.2mg/$m^2$). A half (47.7%) were male sex, one fifth (23%) were current smokers and 16.3% had self-reported hypertension or were on anti-hypertensive medication. Mean QRS duration was 91±11ms and

mean QTc interval was 408±18ms. Mean values of GSfull-wall was -21.1±2.5%, while mean mechanical dispersion was 33.6±11.7ms.

**Association of QRS duration and QT duration with standard echocardiographic parameters**

Subjects with longer QRS (increased QRS delay) duration had lower LVEF (Q-QRS=65.9±6.2 vs. Q4-QRS=64.3±6.5; *P*<0.014), higher LVEDV (Q1-QRS=80.2±20.3 vs. Q4-QRS=104.3±27.7; *P*<0.001) and higher LV mass index (Q1-QRS=78.4±22.7 vs. Q4-QRS =93.6±29.3; *P*<0.001). LA volume index was higher in the highest QRS duration quartile (Q1-QRS=21.1±6.4 vs. Q4-QRS=24.0±7.7; *P*<0.001) (**Table 1**).

LVEF did not differ across QTc quartiles (P=0.13). LV end-diastolic volume, LV mass index and left atrial (LA) volume index were higher in the highest QTc quartile (all *P*<0.05). Mean e' was lower in the highest QTc quartile (Q1-QTc=12.1±3.2 vs. Q4-QTc=11.0±3.0, *P*<0.05) (**Table 1**).

**Association between QRS duration (QRS delay) and myocardial deformation**

Strain parameters (GSfull-wall) showed a stepwise decrease across QRS quartiles (all *P*<0.0001) showing significant worst values in the highest quartile compared to the first two quartiles (*P* <0.05 for comparison between Q4-Q1 and Q4-Q2) (**Table 2**); a significant inverse correlation was observed between each of these parameters and QRS delay (*P*<0.0001) (**Table S1**). The same significant pattern across quartiles was observed for ESS (**Table 2**). PSI did not show any significant differences across QRS quartiles. A non-significant pattern across quartiles also emerged with respect to time-to-peak strain and MD parameters (**Table 2 & Figure 3**).

**Association between QT duration (repolarization delay) and myocardial deformation**

Contrary to the QRS results, specific strain parameters showed a stepwise increase across QTc quartiles (*P*<0.0001) with significant better values in the fourth quartile (*P* <0.05*) (***Table 2**). Significant positive correlations were observed (*P*<0.0001) (**Table S1**). Similar results were found for ESS.

All time-to-peak strain parameters significantly increased in a progressive manner across QTc quartiles (all *P* <0.0001) with significantly better values in the fourth QTc quartile compared to the

first two quartiles (*P* for Q4-Q1 and Q4-Q2 comparisons <0.05) (**Table 2**); this significant relationship was also confirmed by significant positive correlations (*P*<0.0001) (**Table S1**). The same trend was observed for all MD parameters **(Table 2 & Table S1)**

Normal distribution values by QTc tertiles and sex difference are provided in **Table 3**.

**Discussion**

By measuring myocardial deformation patterns in a large population, our results showed that:1) patients with increased QRS duration had lower LVEF and peak systolic strain but no significant relationship with regard to timing and dispersion; 2) patients with longer QTc had a significant delayed time-to-peak strain (about 30ms) associated with an increase in mechanical dispersion. These data thus provide the distribution and range of myocardial deformation parameters according to QTc by sex in a population study.

In addition, in this population-based setting that QRS is not associated with mechanical dispersion, our results suggest that echocardiographic-based dyssynchrony does not largely overlap with ECG-based dyssynchrony. This further supports systematically using imaging to assess dyssynchrony given that the latter is apparently not assessable with routine ECG.

**LV mechanics and intraventricular conduction**

It is readily acknowledged that cardiac electrical conduction, and cardiomyocyte depolarization culminate in mechanical contraction (excitation-contraction coupling) (1). Mechanical alterations in patients with pathological conduction have been widely described, mainly in heart failure (14,19), as well as in patients with left ventricular hypertrophy (20). An increase in QRS delay leads to mechanical dyssynchrony both between and within the ventricles, a largely-studied phenomenon at the basis of cardiac resynchronization therapy (21). In healthy subjects, peak longitudinal strain should occur simultaneously with AVC, with no or only mild post-systolic shortening. Moreover, the peak of strain should also occur simultaneously for the 17 segments with negligible MD. Of particular interest, we did not observe any relationship between QRS duration and MD or with the time-to-peak strain. Delayed QRS is associated with two pathophysiological phenomena: electrical dyssynchrony and LV hypertrophy (1,15,22). However, in the presence setting, given that our patient cohort did not include

patients with QRS over 120ms, it is thus possible to speculate that in patients with normal QRS length, the contribution of QRS to overall mechanical dispersion is minimal.

ECG is the expression of whole heart depolarization and repolarization currents in which their variations in magnitude and timing are reflected by changes in ECG morphology (23).

We found that patients with increased QRS duration had lower LVEF and peak systolic strain. As a potential marker of cardiovascular aging and LV/left atrium cavity remodeling, higher LV mass and higher LA volume indices were also observed, which may be related to preclinical diastolic dysfunction (24).

**LV mechanics and repolarization delay**

Historically, prolonged contraction duration and spatial dispersion of contraction duration were the first alterations identified and initially measured by M mode in patients with long QT syndrome (25,26) (Online ref.1,2). In later studies, tissue Doppler imaging (Online ref.3)(27) and speckle tracking strain analysis (Online ref.4,5)(28), allowed assessing electromechanical changes in this syndrome.

In the present study, patients with longer QT had a more prolonged and heterogeneous contraction resulting in higher post-systolic contraction and mechanical dispersion (Online ref.6), thus highlighting the relationship between repolarization duration and dispersion with MD measured by 2D speckle tracking. These findings are in line with a recent study by Sauer et al. showing significant linear association between ECG repolarization heterogeneity (as T wave peak to T wave end) with mechanical dyssynchrony in 82 patients without QT disorders and without significant cardiomyopathy (Online ref.7). The relationship between mechanical dispersion and prolonged QTc may also be associated with myocardial disarrangement as documented by Hurtado-de-Mendoza et al. who showed a correlation between diffuse interstitial fibrosis assessed by T1 relaxation times in cardiac magnetic resonance and QT dispersion in hypertrophic cardiomyopathy (HCM) patients (Online ref.8). QTc prolongation along with MD has moreover been linked to chronically ischemic myocardium and an increased likelihood of coronary artery disease (Online ref.9).

Interestingly, patients herein with longer QTc showed slightly albeit significantly better peak strain values. This finding, together with the lack of relationship between LVEF and QTc interval,

may be explained by the fact that a more prolonged depolarization provides more time for myocardial contraction, which may correlate with better strain values in healthy subjects. The latter contrasts with findings in patients with long QT syndrome in which a small but significantly worst GLS was found when compared with healthy subjects (28).

According to the present findings, QTc had a more robust relationship with STE-derived temporal parameters than QRS, especially with regard to the delay between electrical activation and peak of deformation. Of note, MD parameters where higher in patients with longer QTc with no relationship with QRS, likely indicating that a longer QRS is likely better correlated with dyssynchrony and not necessarily with prolonged contraction while QTc is the direct measurement of global depolarization duration, including dyssynchrony and prolonged contraction (Online ref.10).

**Clinical Implications**

Traditionally, isolated LVEF is considered as the predominant parameter for sudden cardiac death (SCD) risk stratification and also as a gatekeeper for resynchronization therapy (2); however, in non-ischemic heart failure, this marker failed to select those who may benefit from implantable cardioverter defibrillator (ICD) in primary prevention of SCD (4). Therefore, novel risk-stratification based on echocardiography is needed (4)(Online ref.11). In the current study, we found no association between QRS and mechanical dyssynchrony assessed by myocardial deformation imaging (Online ref.12), it would appear that the latter has no strong overlap with ECG analysis and may consequently have additional prognostic value on top of QRS data in patients with heart failure. This additional prognostic value would none the less necessitate further evaluation in dedicated studies.

The description of reference values and ranges according to electrical activation of the myocardium in the general population represents a first step in improving awareness of the abnormal LV deformation pattern in myocardial disease. Consequently, we believe the present findings will improve comprehension of electromechanical coupling.

Understanding the interactions between QRS, repolarization and mechanical dyssynchrony will furthermore optimize the application of cardiac resynchronization therapy by improving both patient selection and monitoring (21). Indeed, STE provides a practical tool for myocardial mechanics

and cardiac synchronism analysis (19) which is not redundant with routine ECG analysis (as highlighted above).

**Study Limitations**

Given that QRS durations had little variation between patients (91 ± 10.8ms) in this study, our results cannot be extrapolated to the general population. Subclinical left ventricular hypertrophy may partly explain the results in the higher quartile since impaired systolic and diastolic function was noted in this group.

Since QT interval also includes QRS duration, its length can be overestimated in patients with prolonged QRS (Online ref.8,13,14) and it is therefore important to cautiously interpret the conclusions when a relationship with both QRS and QTc is found in the same direction. In a similar manner, a relationship with QRS and QTc going in opposite directions or only toward one of the latter can be interpreted as a more robust finding.

**Conclusion**

Physiological variability in QRS and QTc intervals are associated with subtle but significant changes in myocardial deformation patterns. Better longitudinal strain parameters and increased mechanical dyssynchrony relate to longer QTc and increased QRS delay. Integrating the impact of ventricular, repolarization conduction delay, myocardial mechanics and synchrony is likely to improve our understanding of electromechanical coupling.

**References**

1. Pfeiffer ER, Tangney JR, Omens JH, McCulloch AD. Biomechanics of cardiac electromechanical coupling and mechanoelectric feedback. J Biomech Eng. 2014 Feb;136(2):021007.

2. Priori SG, Blomström-Lundqvist C, Mazzanti A, Blom N, Borggrefe M, Camm J, et al. 2015 ESC Guidelines for the management of patients with ventricular arrhythmias and the prevention of sudden cardiac death: The Task Force for the Management of Patients with Ventricular Arrhythmias and the Prevention of Sudden Cardiac Death of the European Society of Cardiology (ESC). Endorsed by: Association for European Paediatric and Congenital Cardiology (AEPC). Eur Heart J. 2015 Nov 1;36(41):2793–867.

3. Seegers J, Bergau L, Tichelbäcker T, Malik M, Zabel M. ICD risk stratification studies - EU-CERT-ICD and the European perspective. J Electrocardiol. 2016 Dec;49(6):831–6.

4. Køber L, Thune JJ, Nielsen JC, Haarbo J, Videbæk L, Korup E, et al. Defibrillator Implantation in Patients with Nonischemic Systolic Heart Failure. N Engl J Med. 2016 Sep 29;375(13):1221–30.

5. Teodorescu C, Reinier K, Uy-Evanado A, Navarro J, Mariani R, Gunson K, et al. Prolonged QRS duration on the resting ECG is associated with sudden death risk in coronary disease, independent of prolonged ventricular repolarization. Heart Rhythm. 2011 Oct;8(10):1562–7.

6. Tse G, Yan BP. Traditional and novel electrocardiographic conduction and repolarization markers of sudden cardiac death. Eur Eur Pacing Arrhythm Card Electrophysiol J Work Groups Card Pacing Arrhythm Card Cell Electrophysiol Eur Soc Cardiol. 2017 May 1;19(5):712–21.

7. Gorcsan J, Tanaka H. Echocardiographic assessment of myocardial strain. J Am Coll Cardiol. 2011 Sep 27;58(14):1401–13.

8. Mor-Avi V, Lang RM, Badano LP, Belohlavek M, Cardim NM, Derumeaux G, et al. Current and evolving echocardiographic techniques for the quantitative evaluation of cardiac mechanics: ASE/EAE consensus statement on methodology and indications endorsed by the Japanese Society of Echocardiography. Eur J Echocardiogr J Work Group Echocardiogr Eur Soc Cardiol. 2011 Mar;12(3):167–205.

9. Kalam K, Otahal P, Marwick TH. Prognostic implications of global LV dysfunction: a systematic review and meta-analysis of global longitudinal strain and ejection fraction. Heart Br Card Soc. 2014 Nov;100(21):1673–80.

10. Hamada S, Schroeder J, Hoffmann R, Altiok E, Keszei A, Almalla M, et al. Prediction of Outcomes in Patients with Chronic Ischemic Cardiomyopathy by Layer-Specific Strain Echocardiography: A Proof of Concept. J Am Soc Echocardiogr Off Publ Am Soc Echocardiogr. 2016 May;29(5):412–20.

11. Huttin O, Marie P-Y, Benichou M, Bozec E, Lemoine S, Mandry D, et al. Temporal deformation pattern in acute and late phases of ST-elevation myocardial infarction: incremental value of longitudinal post-systolic strain to assess myocardial viability. Clin Res Cardiol Off J Ger Card Soc. 2016 Oct;105(10):815–26.

12. Haugaa KH, Smedsrud MK, Steen T, Kongsgaard E, Loennechen JP, Skjaerpe T, et al. Mechanical Dispersion Assessed by Myocardial Strain in Patients After Myocardial Infarction for Risk Prediction of Ventricular Arrhythmia. JACC Cardiovasc Imaging. 2010 Mar;3(3):247–56.

13. Hasselberg NE, Haugaa KH, Bernard A, Ribe MP, Kongsgaard E, Donal E, et al. Left ventricular markers of mortality and ventricular arrhythmias in heart failure patients with cardiac resynchronization therapy. Eur Heart J Cardiovasc Imaging. 2016 Mar;17(3):343–50.

14. Shimamoto S, Ito T, Nogi S, Kizawa S, Ishizaka N. Left Ventricular Mechanical Discoordination in Nonischemic Hearts: Relationship with Left Ventricular Function, Geometry, and Electrical Dyssynchrony. Echocardiogr- J Cardiovasc Ultrasound Allied Tech. 2014 Oct;31(9):1077–84.

15. Sharma RK, Volpe G, Rosen BD, Ambale-Venkatesh B, Donekal S, Fernandes V, et al. Prognostic implications of left ventricular dyssynchrony for major adverse cardiovascular events in asymptomatic women and men: the Multi-Ethnic Study of Atherosclerosis. J Am Heart Assoc. 2014 Aug 4;3(4).

16. Ferreira JP, Girerd N, Bozec E, Mercklé L, Pizard A, Bouali S, et al. Cohort Profile: Rationale and design of the fourth visit of the STANISLAS cohort: a familial longitudinal population-based cohort from the Nancy region of France. Int J Epidemiol. 2018 01;47(2):395–395j.

17. Coiro S, Huttin O, Bozec E, Selton-Suty C, Lamiral Z, Carluccio E, et al. Reproducibility of echocardiographic assessment of 2D-derived longitudinal strain parameters in a population-based study (the STANISLAS Cohort study). Int J Cardiovasc Imaging. 2017 Sep;33(9):1361–9.

18. Postema PG, Wilde AAM. The measurement of the QT interval. Curr Cardiol Rev. 2014 Aug;10(3):287–94.

19. Chen Z, Hanson B, Sohal M, Sammut E, Jackson T, Child N, et al. Coupling of ventricular action potential duration and local strain patterns during reverse remodeling in responders and nonresponders to cardiac resynchronization therapy. Heart Rhythm. 2016 Sep;13(9):1898–904.

20. Lin X, Liang H-Y, Pinheiro A, Dimaano V, Sorensen L, Aon M, et al. Electromechanical relationship in hypertrophic cardiomyopathy. J Cardiovasc Transl Res. 2013 Aug;6(4):604–15.

21. Brignole M, Auricchio A, Baron-Esquivias G, Bordachar P, Boriani G, Breithardt O-A, et al. 2013 ESC Guidelines on cardiac pacing and cardiac resynchronization therapy: the Task Force on cardiac pacing and resynchronization therapy of the European Society of Cardiology (ESC). Developed in collaboration with the European Heart Rhythm Association (EHRA). Eur Heart J. 2013 Aug;34(29):2281–329.

22. Chan DD, Wu KC, Loring Z, Galeotti L, Gerstenblith G, Tomaselli G, et al. Comparison of the relation between left ventricular anatomy and QRS duration in patients with cardiomyopathy with versus without left bundle branch block. Am J Cardiol. 2014 May 15;113(10):1717–22.

23. Cardone-Noott L, Bueno-Orovio A, Mincholé A, Zemzemi N, Rodriguez B. Human ventricular activation sequence and the simulation of the electrocardiographic QRS complex and its variability in healthy and intraventricular block conditions. Eur Eur Pacing Arrhythm Card Electrophysiol J Work Groups Card Pacing Arrhythm Card Cell Electrophysiol Eur Soc Cardiol. 2016 Dec;18(suppl 4):iv4–15.

24. Nagueh SF, Smiseth OA, Appleton CP, Byrd BF, Dokainish H, Edvardsen T, et al. Recommendations for the Evaluation of Left Ventricular Diastolic Function by Echocardiography: An Update from the American Society of Echocardiography and the European Association of Cardiovascular Imaging. Eur Heart J Cardiovasc Imaging. 2016 Dec;17(12):1321–60.

25. Nador F, Beria G, De Ferrari GM, Stramba-Badiale M, Locati EH, Lotto A, et al. Unsuspected echocardiographic abnormality in the long QT syndrome. Diagnostic, prognostic, and pathogenetic implications. Circulation. 1991 Oct;84(4):1530–42.

26. De Ferrari GM, Nador F, Beria G, Sala S, Lotto A, Schwartz PJ. Effect of calcium channel block on the wall motion abnormality of the idiopathic long QT syndrome. Circulation. 1994 May;89(5):2126–32.

27. Haugaa KH, Edvardsen T, Leren TP, Gran JM, Smiseth OA, Amlie JP. Left ventricular mechanical dispersion by tissue Doppler imaging: a novel approach for identifying high-risk individuals with long QT syndrome. Eur Heart J. 2009 Feb;30(3):330–7.

28. Haugaa KH, Amlie JP, Berge KE, Leren TP, Smiseth OA, Edvardsen T. Transmural differences in myocardial contraction in long-QT syndrome: mechanical consequences of ion channel dysfunction. Circulation. 2010 Oct 5;122(14):1355–63.

**Figure 1. Longitudinal Strain Curves Measured by Speckle Tracking Echocardiography with Deformation Pattern of a Segment normal segment with Transmural Strain GLScalculation (left panel) , an abnormal Segment (Red Curve) with late and post systolic strain (mid panel, ESS: end systolic strain, PSS :post systolic strain )) and mechanical dispersion (MD) calculation (right panel ,:standard derivation of the time to peak of the 17 segments)**

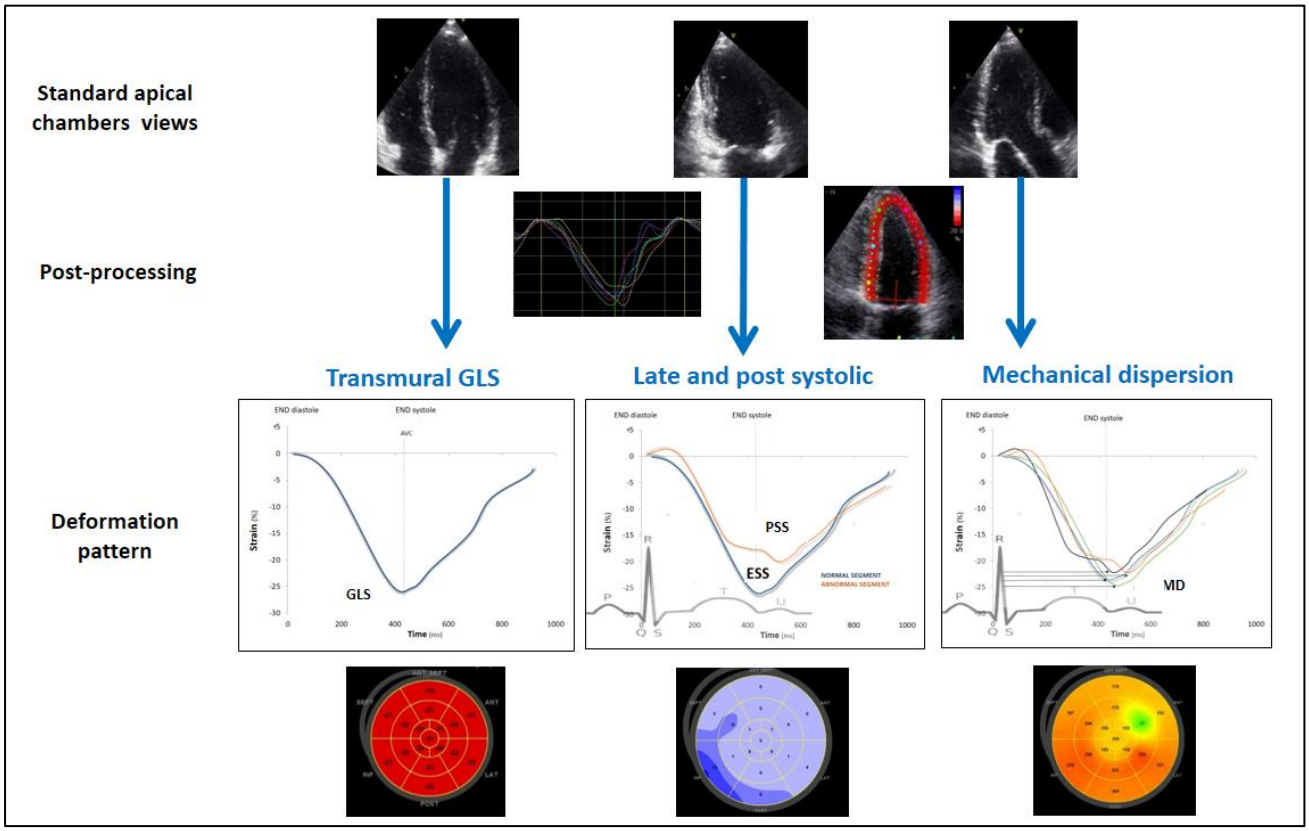

**Figure 2. (Central figure) Radar charts according to quartiles of QRS and QTc delays illustrating the differences in standard echocardiographic and deformation parameters. Values in each group were expressed as z-scores (SD).**

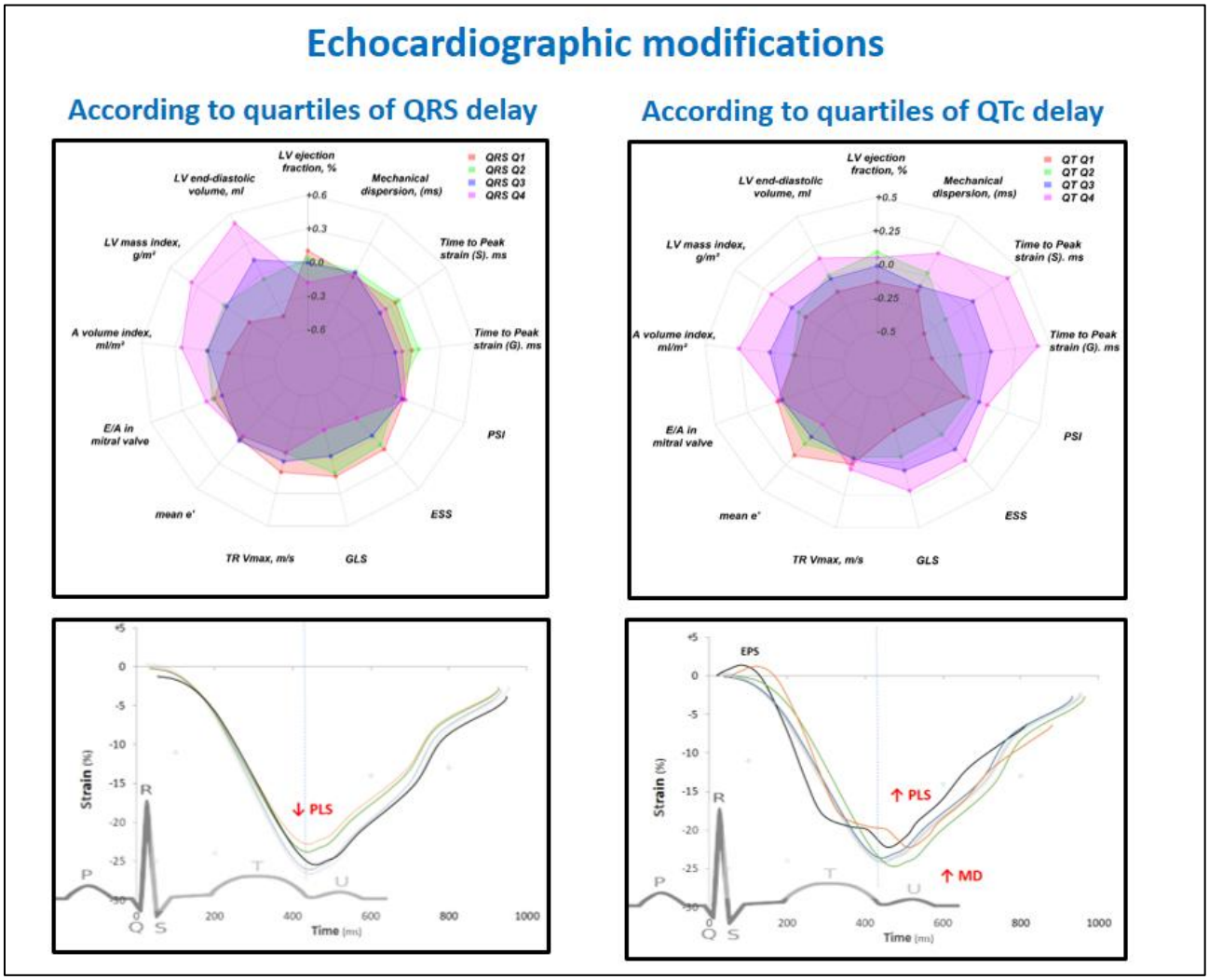

**Figure 3. Heat map based on non-parametric correlations of electrical variables, standard echocardiographic variables and deformation echocardiographic variables.**

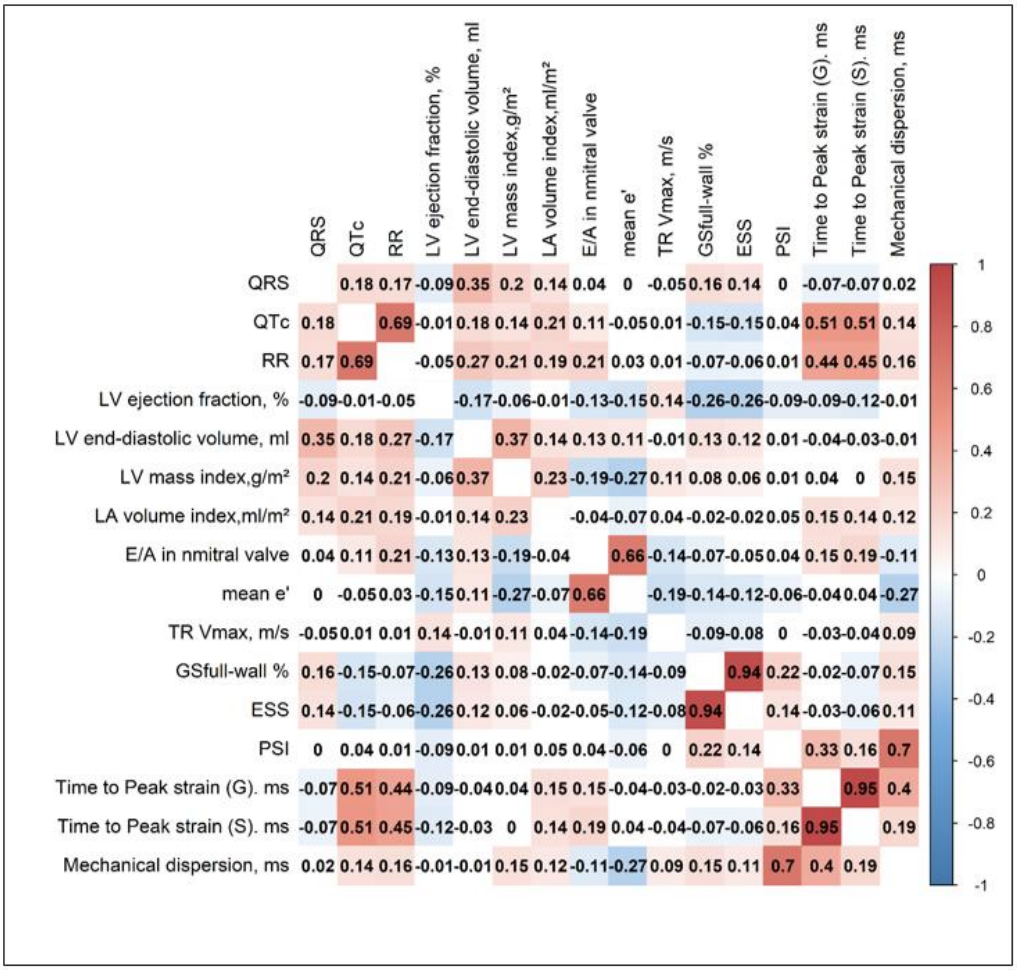

**Table 1. Distribution of Clinical and Standard Echocardiographic Parameters according to QRS and QT Delay Quartiles**

§ P<0.05 vs. Q2 † P<0.05 vs. Q3.

Kruskal Wallis test for nonnormally variable and Bonferonni for nonnormally distributed variables

LV: left ventricular; LA: left atrium; TR Vmax: maximum velocity of tricuspid regurgitation.

**Table 2. Distribution of Myocardial Deformation Parameters according to QRS and QT Delay Quartiles**

GSfull-wall: global peak longitudinal systolic strain full-wall myocardium; ESS: end-systolic peak longitudinal strain; PSI: post-systolic index (n° of abnormal segments); G: global, S: systolic, P: positive, MD: mechanical dispersion.

**Table 3. Normal Distribution of Myocardial Deformation Parameters according to QTc Tertiles by Sex**

GSfull-wall: global peak longitudinal systolic strain full-wall myocardium; ESS: end-systolic peak longitudinal strain; PSI: post-systolic index (n° of abnormal segments); G: global, S: systolic, P: positive, MD: mechanical dispersion

**Table 1: Distribution of Clinical and Standard Echocardiographic Parameters according to QRS and QT Interval Quartiles**

| | QRS (ms) | | | | | QTc (ms) | | | | |
|---|---|---|---|---|---|---|---|---|---|---|
| **Quartile** | **Q1 [0-84]** | **Q2[84-90]** | **Q3[90-96]** | **Q4[96-120]** | **p-value** | **Q1[0-396]** | **Q2[396-407]** | **Q3[407-421]** | **Q4[421-470]** | **p-value** |
| **General characteristics** | | | | | | | | | | |
| **Age, yrs** | 49.3 ± 13.3 | 49.3 ± 14.5 | 47.1 ± 14.0 | 48.4 ± 14.1 | 0.220 | 45 ± 14.5 | 47.7 ± 14.1 | **49.3 ± 13.4**$^{*}$ | **52.4 ± 12.8**$^{*\S\ \dagger}$ | <0.001 |
| **Body mass index, kg/m²** | 25.1 ± 4.4 | 25.4 ± 4.2 | 25.7 ± 4 | 25.7 ± 4.1 | 0.184 | 25.7 ± 4.5 | 25.8 ± 4.1 | 25.3 ± 4.2 | 25 ± 3.9 | 0.125 |
| **Systolic blood pressure, mmHg** | 125.4 ± 16.4 | 128.4 ± 16.5 | 126.6 ± 13.4 | **130.8 ± 14**$^{*\dagger}$ | <0.001 | 129.5 ± 16.3 | 126.9 ± 14.3 | 127.4 ± 15.9 | 127 ± 14.7 | 0.132 |
| **Heart rate, bpm** | 60.6 ± 8.3 | 59.6 ± 7.9 | 61.1 ± 9.2 | **58.9 ± 7.1**$^{*}$ | 0.009 | 60 ± 8.1 | 60.5 ± 8.7 | 60 ± 7.9 | 59.7 ± 8 | 0.699 |
| **Standard echocardiography** | | | | | | | | | | |
| **LV ejection fraction, %** | 65.9 ± 6.2 | 65.5 ± 5.6 | 65.2 ± 6 | **64.3 ± 6.5**$^{*}$ | 0.014 | 64.5 ± 6.3 | 65.7 ± 5.9 | 65.3 ± 5.8 | 65.5 ± 6.3 | 0.129 |
| **LV end-diastolic volume, ml** | 80.2 ± 20.3 | 90.1 ± 25.5$^{*}$ | **95.2 ± 25.7**$^{*}$ | **104.3 ± 27.7**$^{*\dagger\S}$ | <0.001 | 88.1 ± 23.7 | 91.7 ± 28.3 | 91.1 ± 24.7 | **95.7 ± 27.8**$^{*}$ | 0.008 |
| **LV mass index, g/m²** | 78.4 ± 22.7 | 85 ± 24$^{*}$ | **84.9 ± 22.9**$^{*}$ | **93.6 ± 29.3**$^{*\S\dagger}$ | <0.001 | 81.2 ± 21.9 | 84.5 ± 24.5 | 84.9 ± 22.7 | **89.5 ± 30.6**$^{*}$ | 0.004 |
| **LA volume index, ml/m²** | 21.1 ± 6.4 | 22.5 ± 6.9 | 22.4 ± 6.6 | **24 ± 7.7**$^{*}$ | <0.001 | 21.3 ± 6.2 | 21.4 ± 6.3 | 22.6 ± 7.2 | **24.2 ± 7.6**$^{*\S\ \dagger}$ | <0.001 |
| **E/A in mitral valve** | 1.2 ± 0.42 | 1.21 ± 0.42 | 1.18 ± 0.34 | 1.23 ± 0.41 | 0.594 | 1.21 ± 0.4 | 1.2 ± 0.42 | 1.19 ± 0.36 | 1.22 ± 0.43 | 0.893 |
| **mean e'** | 11.6 ± 3.1 | 11.5 ± 3.2 | 11.7 ± 2.9 | 11.4 ± 3.1 | 0.789 | 12.1 ± 3.2 | 11.7 ± 3.2 | 11.4 ± 3 | **11 ± 3**$^{*}$ | 0.001 |
| **TR Vmax, m/s** | 2.19 ± 0.28 | 2.14 ± 0.27 | 2.16 ± 0.31 | 2.13 ± 0.29 | 0.281 | 2.16 ± 0.27 | 2.15 ± 0.31 | 2.14 ± 0.29 | 2.17 ± 0.28 | 0.807 |

## Table 2: Distribution of Myocardial Deformation Parameters according to QRS and QT Delay Quartiles

| | QRS (ms) | | | | | QTc (ms) | | | | |
|---|---|---|---|---|---|---|---|---|---|---|
| **Quartile** | **Q1 [0-84]** | **Q2[84-90]** | **Q3[90-96]** | **Q4[96-120]** | **p-value** | **Q1[0-396]** | **Q2[396-407]** | **Q3[407-421]** | **Q4[421-470]** | **p-value** |
| **GLOBAL LONGITUDINAL STRAIN VALUES** | | | | | | | | | | |
| **GSfull-wall %** | -21.4 ± 2.6 | -21.4 ± 2.3 | -21 ± 2.4 | **-20.4 ± 2.4*§** | <0.0001 | -20.5 ± 2.5 | -21 ± 2.3 | **-21.3 ± 2.4*** | **-21.6 ± 2.6*§** | <0.0001 |
| **GLOBAL TEMPORAL LONGITUDINAL STRAIN VALUES** | | | | | | | | | | |
| **ESS** | -21.8 ± 2.5 | -21.7 ± 2.3 | -21.4 ± 2.3 | **-21 ± 2.5*§** | <0.0001 | -20.9 ± 2.4 | **-21.5 ± 2.3*** | **-21.7 ± 2.3*** | **-21.9 ± 2.6*** | <0.0001 |
| **PSI** | 2.4 ± 1.6 | 2.3 ± 1.4 | 2.4 ± 1.4 | 2.5 ± 2.1 | 0.577 | 2.3 ± 1.4 | 2.3 ± 1.6 | 2.5 ± 1.7 | **2.5 ± 1.9*§** | 0.103 |
| **ELECTRICAL ACTIVATION DELAY and MECHANICAL DISPERSION** | | | | | | | | | | |
| **Time to Peak strain (G). ms** | 369 ± 32 | 372 ± 58 | 363 ± 33 | 366 ± 32 | 0.070 | 353 ± 58 | 361 ± 29 | **372 ± 29*** | **385 ± 30*§** | <0.0001 |
| **Time to Peak strain (S). ms** | 352 ± 31 | 354 ± 57 | 346 ± 31 | 348 ± 29 | 0.710 | 337 ± 58 | 344 ± 28 | **355 ± 27*§** | **365 ± 27*§†** | <0.0001 |
| **Time to Peak strain (P). ms** | 22 ± 11 | 21 ± 12 | 20 ± 12 | 20 ± 12 | 0.191 | 19 ± 11 | 20 ± 12 | **22 ± 11** | **23 ± 12** | <0.0001 |
| **MD. Peak strain (G)** | 33.2 ± 11.8 | 33.9 ± 12.1 | 33.72 ± 11.8 | 33.73 ± 11.5 | 0.913 | 32.5 ± 11.7 | 33.31 ± 11.9 | **32.9 ± 11.3*§** | **35.9 ± 11.9†** | 0.002 |

. **Table 3. Normal Distribution of Myocardial Deformation Parameters according to QTc Tertiles by Sex**

| | Male | | | | | | | | | Female | | | | | | | | |
|---|---|---|---|---|---|---|---|---|---|---|---|---|---|---|---|---|---|---|
| **QTc (ms)** | **< 400 ms (n = 211)** | | | **400-415 ms (n = 181)** | | | **>415 ms (n = 201)** | | | **< 400 ms (n = 197)** | | | **400-415 ms (n = 202)** | | | **>415 ms (n = 234)** | | |
| | **mean** | **P 5th** | **P 95th** | **mean** | **P 5th** | **P 95th** | **mean** | **P 5th** | **P 95th** | **mean** | **P 5th** | **P 95th** | **mean** | **P 5th** | **P 95th** | **mean** | **P 5th** | **P 95th** |
| **GLOBAL LONGITUDINAL STRAIN VALUES** | | | | | | | | | | | | | | | | | | |
| **GSfull-wall %** | **-20.1** | -23.8 | -16.4 | **-20.7** | -24.5 | -17.1 | **-20.8** | -24.7 | -16.7 | **-21.1** | -25.4 | -17.1 | **-21.7** | -25.9 | -18.1 | **-21.9** | -26.7 | -17.6 |
| **GLOBAL TEMPORAL LONGITUDINAL STRAIN VALUES** | | | | | | | | | | | | | | | | | | |
| **ESS** | **-20.5** | -24.1 | -16.8 | **-21.1** | -25.1 | -17.5 | **-21.1** | -25.0 | -17.3 | **-21.4** | -25.5 | -17.6 | **-22.1** | -25.8 | -18.5 | **-22.3** | -27.1 | -18 |
| **PSI** | **2.52** | 0.51 | 5.61 | **2.58** | 0.41 | 7.19 | **2.75** | 0.57 | 6.40 | **2.49** | 0.58 | 5.34 | **2.67** | 0.54 | 6.00 | **2.97** | 0.58 | 6.19 |
| **ELECTRICAL ACTIVATION DELAY and MECHANICAL DISPERSION** | | | | | | | | | | | | | | | | | | |
| **Time to Peak strain (G). ms** | **358** | 291 | 430 | **372** | 316 | 499 | **391** | 318 | 516 | **378** | 319 | 469 | **387** | 331 | 438 | **401** | 347 | 475 |
| **Time to Peak strain (S). ms** | **327** | 278 | 378 | **338** | 290 | 379 | **354** | 299 | 396 | **351** | 298 | 390 | **358** | 314 | 406 | **371** | 328 | 412 |
| **Time to Peak strain (P). ms** | **19** | 2.2 | 39 | **17.82** | 3 | 38 | **18** | 3.9 | 39 | **23** | 5.2 | 44 | **25** | 6.4 | 45 | **27** | 7.9 | 53 |
| **MD. Peak strain (G)** | **31.9** | 14.2 | 52.9 | **32.5** | 13.0 | 52.7 | **34.9** | 15.5 | 57.9 | **33.1** | 15.7 | 56.6 | **33.9** | 17.7 | 53.8 | **35.2** | 16.6 | 55.8 |